Water-assisted photocatalytic sulfide and alcohol oxidation by a Ru-Ru dyad

Johannes Klein, Stéphane Torelli, Damien Jouvenot, Frédérique Loiseau, Stéphane Ménage, Olivier Hamelin

Water-assisted Photocatalytic Sulfide and Alcohol Oxidation by a Ru-Ru Dyad

Johannes Klein, [a] Stéphane Torelli,*[a] Damien Jouvenot, [b] Frédérique Loiseau, [b] Stéphane Ménage, [a] and Olivier Hamelin*[a]

[a] Univ. Grenoble Alpes, CEA, CNRS, IRIG-LCBM, UMR 5249, 38000, Grenoble, France. E-mail: stephane.torelli@cea.fr; olivier.hamelin@cea.fr.

[b] Univ. Grenoble Alpes, CNRS, DCM; UMR 5250, 38041 Grenoble, France.

Running title: Sun, Water and a photocatalyst: what else for oxidation?

Abstract: Moving toward eco-friendly and eco-environmentally processes to perform specific organic transformations is more than ever at stake. Inspired by Nature that uses light as inducer with PSII, a new Ru-based dyad combining a photosensitizer with a catalytic partner was developed. Upon irradiation with low power consumption blue LEDs, this system has proven its effectiveness during the catalytic oxidation of various sulfides and alcohols with water as unique oxygen atom source.

Keywords: Photocatalysis, dyad, sulfide and alcohol oxidation

Introduction

In the context of the development of eco-friendly and eco-aware chemical processes, oxygenation of organic substrates using renewable, cheap, nontoxic and abundant oxygen atom sources such as water (H_2O) and molecular dioxygen (O_2), is still a challenge, mainly due to the relative inertness of the latter that requires commonly the use of metal cofactors. Additionally, one can easily imagine that if the energy source needed to initiate the overall process comes from light, the above-mentioned considerations would be fully integrated. In this vein, Nature, with photosystem II (PS(II)), has developed a fantastic machinery in order to perform light-driven H_2O oxidation into O_2 and use the liberated electrons to generate the NADPH reducing cofactor involved in the Calvin cycle to assimilate carbon dioxide (CO_2). Consequently, the combination of a light-absorbing photosensitizer with a catalytic partner dedicated to reactions of interest appears to be an inspiring strategy. Numerous systems as models of PS(II) are reported to achieved photocatalytic water oxidation, one of the two steps leading to water splitting. Some of them are Ru-based and involve the formation of an oxidizing high-valent Ru=O intermediate arising from a Ru-OH_2 moiety.[1] Such a species is also known to have the ability to oxidize organic substrates such as alcohols, phosphines, and sulfides.[2-6] However, despite the increasing interest in this area, only few systems are reported to use water as oxygen atom source to perform photocatalytic organic substrate oxidations. Herein, based on a bio-inspired approach, we developed a new homodinuclear ruthenium-based photocatalyst denoted **Ru_{phot}-Ru_{cat}-Cl** (Scheme 1) constituted by *i)* a light-absorbing $[Ru(bpy)_3]^{2+}$-like fragment (bpy = 2,2'-bipyridine, abbreviated **Ru_{phot}**) known to be an efficient photosensitizer and *ii)* a catalytic $[Ru(tpy)(bpy)(Cl)]^+$ fragment (tpy = 2,2':6'2"-terpyridine, abbreviated **Ru_{cat}-Cl**) capable of achieving organic substrate oxidation after *in situ* chlorido displacement by a water molecule.

Material and methods

^1H and ^{13}C NMR spectra were recorded on a Bruker Avance 300 MHz at 298K and processed with the Bruker TopSpin software.
Elemental analyses were conducted at the Institut de Chimie of Strasbourg.
Mass spectrometry spectra were recorded with a Bruker Daltonics Esquire 3000 Plus(ESI-MS) device.
Absorption spectra were recorded with a Shimadzu UV-1800 spectrophotometer.
Electrochemical experiments were performed in MeCN under inert N_2 atmosphere. A three-electrode setup was used, and consists of a glassy carbon (3mm in diameter) disk as a working electrode, a platinum wire serves as auxiliary electrode and an Ag/AgCl/ aqueous $AgCl_{sat}$ + KCl 3 M (hereafter named Ag/AgCl) as reference electrode directly dipped into the solution. Cyclic voltammograms were recorded with a Bio-logic SP-300 potentiostat piloted by the EC-Lab software. All measurements were referenced externally to ferrocene and correspond to the n+1 scan.
Emission spectra were recorded at room temperature on a Varian Cary Eclipse fluorescence spectrophotometer. Samples were placed in 1 cm path length quartz cuvettes. Luminescence lifetimes measurements were performed after irradiation at λ = 400 nm obtained by the second harmonic of a Titanium:Sapphire laser (picosecond Tsunami laser spectra physics 3950-M1BB + 39868-03 pulse picker

doubler) at a 400 kHz and 8 MHz repetition rate. Fluotime 200 from AMS technologies was used for the decay acquisition. It consists of a GaAs microchannel plate photomultiplier tube (Hamamatsu model R3809U-50) followed by a time-correlated single photon counting system from Picoquant (PicoHarp300). The ultimate time resolution of the system is close to 30 ps. Luminescence decays were analyzed with Fluofit software available from Picoquant. Emission quantum yields (ϕ) were determined at room temperature in deoxygenated acetonitrile solutions using the optically dilute method.

$[Ru(bpy)_3]^{2+}$ (bpy = 2,2'-bipyridine) in air-equilibrated aqueous solution was used as quantum yield standard (ϕ = 0.028). [2]

The photochemical photo-oxygenation was performed in a Schlenk tube (10 mm i.d.) containing a mixture of catalyst, substrate and Co(III) salt in a 1(40μM):200:400 ratio in 0.1M phosphate buffer (pH 6.8). After 24 h of irradiation (Blue Led system emitting at 465 nm, 11mW.cm^{-2}), extraction with Et_2O (3 times) then CH_2Cl_2 (3 times) and concentration in vacuum, the products were characterized and quantified by ^{1}H NMR using trimethoxybenzaldehyde as internal reference.

Synthetic details: Solvents for oxygen and/or moisture sensitive reactions were freshly distilled under argon from the appropriate dehydrating agent and degassed with dry nitrogen before use. Solvents for chromatography and work-up procedures were of puriss p.a. grade. For the complexes, a puriFlash machine (30 mL/min) with prepacked columns (either 25 or 40 g) was used. $Ru(bpy)_2Cl_2{\cdot}2H_2O$ and $Ru(dmso)_4Cl_2$ were received from *Strem*. $Ru(bpy)(dmso)_2Cl_2$ was synthesized according to literature procedures. All other chemicals were obtained commercially and used without further purification.

Results and discussion

The executed route to **Ru_{phot}-Ru_{cat}-Cl** is depicted in Scheme 1 and the experimental synthesis details provided in the Supporting information.

It is obvious that the electronic structure of the bridging unit that connects both partners has a direct influence on the catalytic activity notably by influencing the kinetics of the photo-induced electron transfer (PET) between the catalyst and the photosensitizer. Indeed, it has been shown that both highly conjugated and π-acceptor ligands decrease the catalytic activity by increasing charge trapping during the PET.[7, 8] Consequently, with this in mind, the (4'-(4-([2,2'-bipyridin]-5-yl)-2,5-dimethylphenyl)-2,2':6',2''-terpyridine) (**bptp**) ligand constituted by the association of a bipyridine and a terpyridine moieties through a phenyl bridge was designed. It is expected that the tilt angle imposed by the methyl substituents on the phenylene bridge would induce an important distortion from planarity resulting in a conjugation breakdown that should minimize charge recombination.[9]

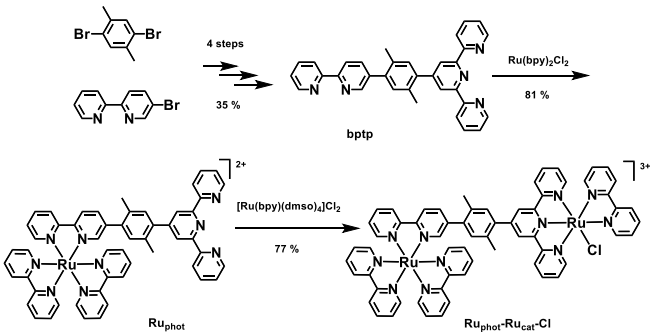

Scheme 1. Executed route to **Ru_{phot}-Ru_{cat}-Cl**.

The bridging **bptp** ligand was readily obtained in 4 steps from 5-Bromo-2,2'-bipyridine [10] and 1,4-Dibromo-2,5-dimethylbenzene *via* Miyaura borylation [11] and Suzuki coupling reaction [12]. Selective formation of the chromophore unit was obtained as a single isomer by condensation of **bptp** with $[Ru(bpy)_2Cl_2]$ and subsequent introduction of the second metal cation using $[Ru(bpy)Cl_2(dmso)_2]$ [8] to afford **Ru_{phot}-Ru_{cat}-Cl** in a reasonable overall yield (22%). For comparison, $[Ru(bptp)(bpy)(Cl)]^+$ (**Ru_{cat}-Cl**) was also prepared (see Supporting information). For the latter, single crystals of its precursor were obtained by vapor diffusion of pentane into an acetone solution of the complex. The X-ray structure (Figure 1) reveals a distorted octahedral geometry around the Ru^{II} cation.

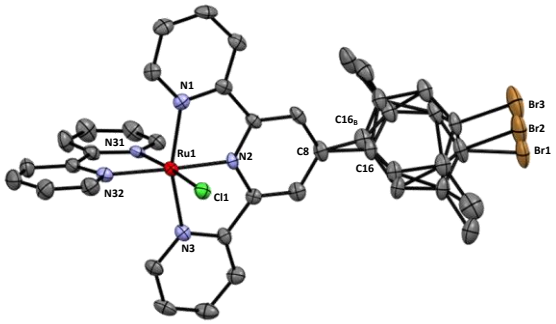

Figure 1. ORTEP diagram of the monocationic unit of **Ru_{cat}-Cl** with all non-H atoms shown as 50% thermal ellipsoids. Selected interatomic distances (Å) and angles (deg): Ru-Cl, 2.4112(12); Ru-N1, 2.056(3); Ru-N2, 1.951(3); Ru-N3, 2.072(3); Ru-N31, 2.028(4); Ru-N32, 2.066(3); N31-Ru-N32, 83.71(17); C8-$C16_B$, 1.380(3); C8-C16, 1.522(3) N32-Ru-Cl, 114.23(17); See Tables S1, S2 and S3 in the Supporting Information for additional details.

The tridentate tpy ligand is coordinated to the metal center *via* the expected meridional mode, its constraint effect being responsible of the pseudooctahedral arrangement. The chlorido coligand is in the *cis* position and the two N atoms from the bpy moiety complete the coordination sphere. The N_{tpy}-Ru bond lengths are in the common range 2.072(3) to 1.951(3) Å, the one for the central N being the shortest.[13] In the same vein, the Ru-Cl bond distance of 2.4112(12) Å falls in the range of other reported Ru(tpy)Cl-containing compounds. [14] For the bidentate bpy ligand, the N_{bpy}-Ru bond lengths differ by 0.038 Å. Due to the *trans*

effect of Cl^-, the Ru-N31 bond length is shortened to 2.028(3) Å while the Ru-N32 (2.066(3) Å) is in the range of other described Ru(bpy)-based structures.[15, 16] Finally, and as expected, the bromodimethylphenyl fragment, although disordered, is twisted from the main tpy plane by *ca*.30° which makes it possible to reduce the conjugation between the two partners of the dyad and thus the charge recombination. As a consequence, the mean C_8-C_{16} bond length of 1.451(3) Å is of intermediate sp^2/sp^3 character.

Cyclic voltammetry (CV) was performed for all complexes in CH_3CN (Figure S1 in the Supporting Information). **Ru_{phot}** shows, in the cathodic region, four successive quasi-reversible one-electron processes between -1.5 V and -2.5 V *vs* $Fc^{+/0}$ corresponding to the reduction of the three bpy ligands and the uncoordinated tpy moiety.[17, 18] The cathodic part exhibits a reversible **$Ru^{II/III}_{phot}$** process at 0.91 V vs $Fc^{+/0}$ (Table 1). Concerning **Ru_{cat}-Cl**, three reduction processes can be observed. Among these, one relies to the bpy moiety while the remaining two correspond to the coordinated tpy. For the latter, the central pyridine ring is reduced at a different redox potential compared to the lateral ones. [19, 20] Here again, the only anodic process detected corresponds to a reversible **$Ru^{II/III}_{cat}$-Cl** event at 0.49 V vs $Fc^{+/0}$ that occurs at lower potential compared to that in **Ru_{phot}** due to the π-donor character of the chlorido ligand. Combining both partners within the same macromolecule in **Ru_{phot}-Ru_{cat}-Cl** results in a CV curve with a cathodic part being extremely complicated and difficult to analyze, with barely reversible events and an electrodeposition phenomenon. The anodic region is more straightforward to interpret since it essentially shows both **$Ru^{II/III}_{phot}$** and **$Ru^{II/III}_{cat}$-Cl** processes at redox potentials (0.93 V and 0.43 V vs $Fc^{+/0}$, respectively) nearly unchanged compared to those evidenced for the independent complexes. Taking into account *(i)* the chlorido/aqua exchange at **Ru_{cat}-Cl** expected to occur under catalytic conditions and *(ii)* the lower oxidation potential for the corresponding Ru_{cat}-OH_2 part due to a proton coupled electron transfer (PCET) compared to Ru_{cat}-Cl,[2] oxidation of Ru^{II}_{cat}-OH_2 by the photogenerated Ru^{III}_{phot} is thermodynamically favored .

Table 1. Electrochemical data for the anodic events determined for **Ru_{phot}-Ru_{cat}-Cl** and as-isolated mononuclear **Ru_{phot}** and **Ru_{cat}-Cl** subunits; $E_{1/2}$ in V *vs* $Fc^{+/0}$ ($\Delta E = E_{ox}-E_{red}$ in millivolts). Solvent: CH_3CN

Ru_{phot}	**Ru_{cat}-Cl**	**Ru_{phot}-Ru_{cat}-Cl**
+0.91 (73) ($Ru^{III}_{phot}/Ru^{II}_{phot}$)	+0.49 (66) ($Ru^{III}_{cat}/Ru^{II}_{cat}$)	+0.43 (84) ($Ru^{III}_{cat}/Ru^{II}_{cat}$) +0.93 (92) ($Ru^{III}_{phot}/Ru^{II}_{phot}$)

The absorption properties of all three complexes were then investigated in acetonitrile. All of them display an intense absorption around 290 nm assigned to ligand centered (^{1}LC) π–π* transitions (Table 2). In the visible region, **Ru_{phot}** shows typical broad absorption bands at 430 and 460 nm characteristic of Ru(diimine)$_3$ complexes and attributed to metal-to-ligand charge transfer transitions (^{1}MLCT).[21] Similarly, **Ru_{cat}-Cl** features ligand centered transitions ranging from 260 to 340 nm as well as a broad MLCT transition centered at 510 nm and extending up to 620 nm in the line of other reported Ru(tpy)-based compounds.[3] The absorption spectrum of **Ru_{phot}-Ru_{cat}-Cl** being a linear combination of both the **Ru_{phot}** and **Ru_{cat}-Cl** contributions, the targeted electronic decoupling between the two subunits tanks to the *p*-xylenyl bridge upon excitation is then established.

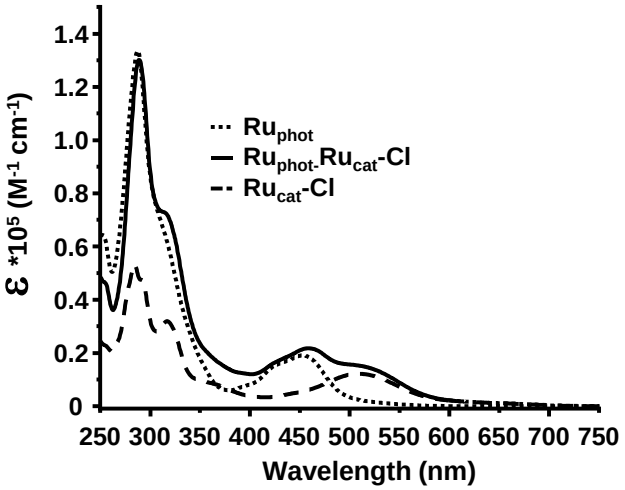

Figure 2. Absorption spectra of **Ru_{phot}**, **Ru_{cat}-Cl** and **Ru_{phot}-Ru_{cat}-Cl** in air equilibrated acetonitrile solutions at room temperature.

Table 2. Spectroscopic data for [**Ru_{phot}**][PF_6]$_2$ (0.1 mM), [**Ru_{cat}-Cl**][PF_6] (10.0 μM) and [**Ru_{phot}-Ru_{cat}-Cl**][PF_6]$_3$ (10.0 μM) in CH_3CN.

	λ_{max}/nm (ε/$M^{-1}.cm^{-1}$)	
	^{1}LC (π→π*)	^{1}MLCT($d\pi_{Ruphot,\ Rucat}\rightarrow\pi^*$)
$[Ru_{phot}]^{2+}$	290(100400)	430(13250)
		455(14350)
$[Ru_{cat}$-Cl$]^+$	285(52000)	510(12150)
	295(46500)	
	290(131000)	430(17550)
$[Ru_{phot}$-Ru_{cat}-Cl$]^{3+}$	315(72800)	460(21700)
		505(15450)$d\pi_{Rucat}\rightarrow\pi^*_{tpy}$

The luminescence of all three complexes was then measured in CH_3CN. As expected, the photosensitizer entity alone exhibits a characteristic emission for tris(diimine)Ru(II) compounds,[22] centered at 610 nm (λ_{ex}= 453 nm), with a mono-exponential lifetime of 1 μs and a quantum yield (Φ) of 0.07 whereas the catalytic entity alone has a particularly weak emission ($\Phi = 2.10^{-5}$) with a lifetime of 17 ns at 730 nm (λ_{ex} = 510 nm). If the **Ru_{phot}-Ru_{cat}-Cl** dyad is excited at low energy (λ_{ex} = 510 nm) the observed spectrum corresponds mainly to the emission of the **Ru_{cat}** part of the molecule. On the other side, upon excitation in the ^{1}MLCT of **Ru_{phot}** (455

nm) the resulting emission features two maxima corresponding to the virtually unchanged emissions of both Ru centers (610 and 730 nm) with comparable intensities. Knowing that the emission quantum yield of **Ru_{phot}** is 3500 times higher than that of **Ru_{cat}**, the fact that they appear to be in the same order of magnitude suggests a quasi-total energy transfer from **Ru_{phot}** to **Ru_{cat}**.

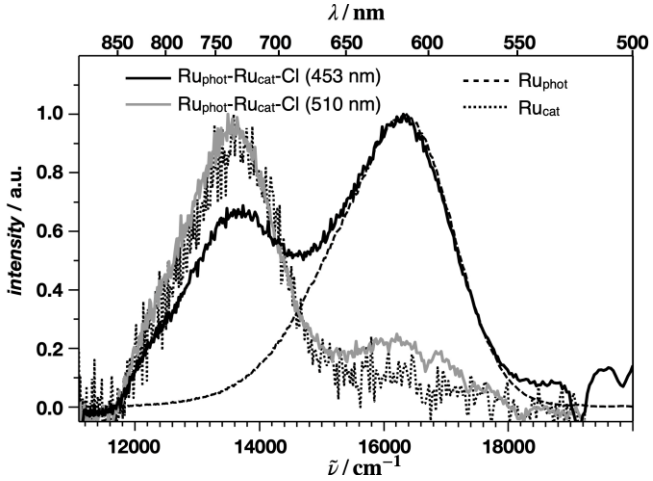

Figure 3. Normalized emission spectra of **Ru_{phot}**, **Ru_{cat}-Cl** and **Ru_{phot}-Ru_{cat}-Cl** excited at 453 nm or 510 nm at the concentration of 10^{-5}M in air equilibrated acetonitrile solutions at room temperature.

It is well known that polypyridine Ru-Cl complexes are not active water oxidation catalysts, but rather pre-catalysts undergoing chlorido/aqua substitution affording the catalytically active Ru-OH_2 species. [1, 23] Oxidation of this latter results in the formation of a highly reactive Ru^{IV}=O species able to oxidize water but also organic substrates.[2-6]

Consequently, the photocatalytic efficiency of the dyad was then evaluated during light-driven oxygenation of 4-bromophenyl methyl sulfide as probe substrate in deoxygenated phosphate buffer at pH 6.8 in the presence of $[Co(NH_3)_5Cl]Cl_2$ as low-cost and weak irreversible one-electron sacrificial acceptor.[24] Irradiation was carried out for 24 h with a blue LED system emitting at 465 nm in the ^{1}MLCT band of **Ru_{phot}** with a light intensity of 11 mW.cm^{-2}. All the photocatalytic experiments were performed under inert atmosphere in order to prevent the photochemical formation of $^1O_2$ as potential oxidant. After extraction, the products were quantified by ^{1}H NMR. In the presence of 200 equiv. of substrate and 400 equiv. of Co(III) salt, up to 63 TON were achieved, affording sulfoxide as a unique oxygenated product. No sulfone could be observed. As expected no product was detected without light irradiation, dyad or cobalt salt. Additional photocatalytic experiments were carried out using either $[Ru(bpy)_3]^{2+}$ as commercial **Ru_{phot}** surrogate or only **Ru_{cat}-Cl** as well as with a 1:1 of $[Ru(bpy)_3]^{2+}$:**Ru_{cat}-Cl** mixture (Table 3). The chromophore alone, though devoided of its catalytic partner, showed a non-negligible catalytic activity (8 TON). This can be explained by the generation of a $[Ru(bpy)_3]^{3+}$ species known to be a stronger one-electron oxidant by photoinduced electron transfer from the $[Ru(bpy)_3]^{2+*}$ excited state to the Co(III) salt.[4] Sulfide oxidation by $[Ru(bpy)_3]^{3+}$ results in the formation of a transient $RS^{\cdot+}$ thiyl radical that further reacts with water, yielding the corresponding sulfoxide.[25, 26] Inversely, up to 48 TON were reached by the catalytic partner alone, as it was observed with other systems.[2] As spectroscopic data of **Ru_{cat}** show an absorption band between 400 and 620 nm corresponding to MLCT transitions, one may assume that LED irradiation at 465 nm results in the generation of a **Ru_{cat}*** photoexcited state as a substitute of the photosensitizer. However, the stoichiometric combination of both constituents ($[Ru(bpy)_3]^{2+}$ and **Ru_{cat}-Cl**) does not lead to the sum of both catalytic activities but rather to an inhibition of the **Ru_{cat}** activity. This feature is still unexplained. Consequently, these results show, once again, the interest to associate both partners within a dyad compared to the bimolecular system.

Table 3. Photocatalytic oxidation of 4-bromophenyl methyl sulfide.

Compound	[**Ru_{phot}-Ru_{cat}-Cl**]$^{3+}$	$[Ru(bpy)_3]^{2+}$	Ru_{cat}	$[Ru(bpy)_3]^{2+}$ + Ru_{cat} [g]
TON	63[a], 0[b] 41[c], 19[d], 22[e], 40[f]	8[a]	48[a]	11[a]

Complex:Substrate:Co(III) ratio 1(40 μM):200:400 in a deoxygenated 0.1M phosphate buffer (pH 6.8) for 24 h; [a] blue LED irradiation (465 nm; light intensity 11mW.cm^{-2}; [b] in the absence of light; [c] in the presence of 200 equiv of Co (III); [d] 800 equiv. of Co(III); [e] 1200 equiv. of Co(III); [f] presence of acetone (10 %); [g] $[Ru(bpy)_3]^{2+}$= $[Ru_{cat}]$ =20 μM

Then, additional experiments were carried out in order to benchmark the catalytic properties of the dyad. First, the effect of the Co(III) salt concentration was investigated (Table 1) and shows that an increase in concentration of more than 400 equiv. (16 mM) with regard to the catalyst leads to a drop of the activity. This observation can be the consequence of the strong absorption of the highly concentrated electron acceptor at the irradiation wavelength (ε = 30 M^{-1}.cm^{-1} at 465 nm) decreasing the intensity of the scattered light within the solution.

Even the presence of 10% of acetone as co-solvent in the reaction mixture to increase the solubility of the substrate did not improve the activity since only 40 TON were achieved.

The influence of light intensity on the catalytic activity was then studied. As seen in Figure 4, an optimized condition is reached with a light intensity of about 12 mW.cm^{-2} with 60-65 TON. As it was observed that similar dyads combining a $Ru(diimine)_3$ photosensitizer with a catalytic subunit decomposed progressively upon

illumination,[2] it can be assumed that too powerful irradiation accelerates the degradation of the complex resulting in lower activities.

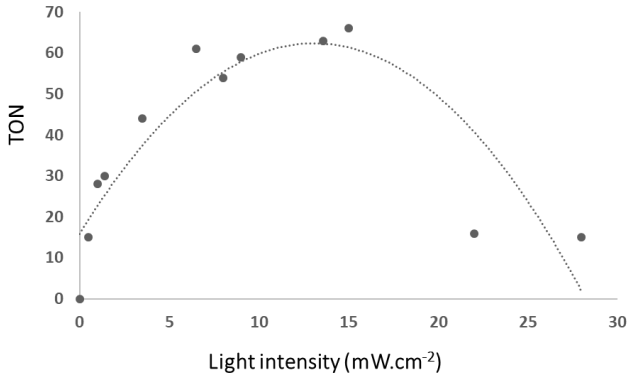

Figure 4. Bell-shape curve for the evolution of the TON for **Ru_{phot}-Ru_{cat}-Cl** as a function of light intensity.

In such optimized conditions (complex:substrate:Co(III) ratio 1:200:400 ; blue LED irradiation (465 nm; light intensity 11mW.cm^{-2})), the photocatalytic activity of **Ru_{phot}-Ru_{cat}-Cl** was evaluated for the oxidation of a variety of sulfides and alcohols (Table 4). As expected, while electron withdrawing groups decrease the reactivity of the sulfides (only 6 TON when R = -CO_2H), electron donating substituents allow to considerably increase the catalytic efficiency with up to 145 TON with R = -OMe (73 % conversion). In all cases, the oxidation proved to be highly selective since no sulfones as over-oxidized products were detected. Photocatalytic oxidation of benzylic alcohol is also highly selective since the corresponding aldehyde was formed as the unique product but, however, with a moderate efficiency (up to 35 TON). Finally, oxidation of (4-(methylthio)phenyl)methanol having both sulfide and primary hydroxyl groups was achieved. The chemoselectivity is in favor of the sulfide with up to 56 TON compared to 21 TON for the alcohol. Only a small proportion of the substrate could be oxidized on both positions. Indeed, the oxidation of one or the other group leads to the introduction of a deactivating electro-withdrawing substituent (sulfoxide or aldehyde) with the effect on the reactivity described above.

Table 2. Photocatalytic oxidation of a variety of sulfides and alcohols.[a]

Substrate	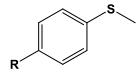				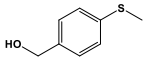	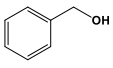
R	H	Br	CO_2H	OMe		
TON	44	63	6	145	21 (S+CHO) 56 (SO+OH) 3 (SO+CHO)	35 (CHO)

[a] **Ru_{phot}-Ru_{cat}-Cl**:Substrate: Co(III) ratio 1(40 μM):200:400 in a deoxygenated 0.1M phosphate buffer (pH 6.8) for 24h; blue LED irradiation (465 nm; light intensity 11mW.cm^{-2}).

Conclusion

In conclusion, we synthesized and fully characterized a new homodinuclear ruthenium-based dyad combining a photosensitizer and a catalytic partner. The bridging dimethylphenylene ligand confers a significant distortion from planarity between the two subunits which minimizes inherent charge recombination. The reported dyad, which proved to be more efficient compared to the bimolecular system, shows reasonable catalytic activity toward light-driven sulfides (up to 145 TON) and alcohol oxidation. In both cases the selectivity is good since no over-oxidized product could be detected. Importantly, during this study we also demonstrated the influence of light intensity on the catalytic efficiency (bell-shape curve with a maximum at 11mW.cm^{-2}). Consequently, in order to optimize such light-driven activity, in the future, it is important not to neglect this parameter during the development of new photocatalytic systems.

Acknowledgements

The authors gratefully acknowledge the ARCANE Labex (CBH-EURGS ANR-17-EURE-0003). This study was also supported by the ANR program (TROICAT, ANR-15-CE07-0025-01). We thank Dr J. Pécaut for collecting the X-ray data on **Ru_{cat}-Cl**.

Conflict of interest

There are no conflicts to declare.

Supporting information for this article is given via a link at the end of the document.

References

1. Kamdar, J. M. and Grotjahn, D. B., 2019, Molecules, 24, 494 and references cited therein.
2. Hamelin, O., Guillo, P., Loiseau, F., Boissonnet M.-F. and Ménage, S. 2011, Inorg. Chem. 50, 7952.
3. Li, T. T., Li, F.-M., Zhao, W.-L, Tian Y.-H., Chen Y., Cai, R. and Fu, W.-F. 2015 Inorg.Chem., 54, 183.
4. Fukuzumi, S., Kojima, T., Lee, Y.-M. and Nam, W. 2017, Coordination Chem. Rev., 333, 44.
5. Ohzu, S., Ishizuka, T., Hirai, Y., Fukuzumi and S., Kojima, T. 2013, Chem. Eur. J., 19, 1563.
6. Li, F., Yu, M., Jiang, Y., Huang, F., Li Y., Zhang, B. and Sun, L. 2011, Chem. Commun., 47, 8949.
7. Chen, W., Rein, F. N., Scott, B. L. and Rocha, R. C. 2011, Chem. Eur. J., 17, 5595.
8. Li, T.-T., Li, F.-M., Zhao, W.-L., Tian, Y.-H., Chen, Y., Cai, R. and Fu, W.-F. 2015, Inorg. Chem., 54, 183.
9. Hankache, J. and Wenger, O. S. 2011, Chem. Commun., 47, 10145.

10. Heinz, L. G., Yushchenko, O., Neuburger, M., Vauthey, E. and Wenger, O. S. 2015, J. Phys. Chem. A, 119, 5676.
11. Farran, R., Jouvenot, D., Gennaro, B., Loiseau, F., Chauvin, J. and Deronzier, A. 2016, ACS Appl. Mater. Interfaces, 8, 16136.
12. Orazietti, M., Kuss-Petermann, M., Hamm, P. and Wenger, O. S. 2016, Angew. Chem. Int. Ed., 55, 9407.
13. Patra, S., Sarkar, B., Ghumaan, S., Patil, M. P., Mobin, S. M., Sunoj, R. B., Kaim, W. and Lahiri, G. K. 2005, Dalton trans., 1188 and ref cited therein.
14. Wanniarachchi, D. C., Heeg, M. J. and Verani, C. N. 2014, Inorg. Chem, 3311 and ref cited therein.
15. Hua,S.-A., Cattaneo, M., Oelschlegel, M., Heindl, M., Schmid L., Dechert S., Wenger O. S., Siewert I., González, L. and Meyer, F. 2020, Inorg. Chem. 59, 7, 4972.
16. Heuer, W. B., Xia, H.-L., Ward, W., Zhou, Z., Pearson, W. H., Siegler, M. A., Sarjeant, A. A. N., Abrahamsson, M. and Meyer, G. J. 2012, Inorg. Chem. 51, 3981.
17. Calvert, J. M., Schmehl, R. H., Sullivan, B. P., Facci, J. S., Meyer, T. J. and Murray, R. W. 1983, Inorg. Chem., 22, 2151.
18. Tseng, H.-W., Zong, R., Muckerman and J. T., Thummel, R. 2008, Inorg. Chem., 47, 11763.
19. Constable, E. C. and Thompson, A. M. W. C. 1994, J. Chem. Soc., Dalton Trans., 1409.
20. Figgemeier, E., Merz, L., Hermann, B. A., Zimmermann, Y. C., Housecroft, C. E., Güntherodt, H.-J. and Constable, E. C. 2003, J. Phys. Chem. B , 107, 5, 1157.
21. Campagna, S., Puntoriero, F., Nastasi, F., Bergamini, G. and Balzani, V., 2007, Photochemistry and Photophysics of Coordination Compounds I, Vol. 280 (Eds.: V. Balzani, S. Campagna), Springer Berlin Heidelberg, pp. 117-214.
22. Juris, A., Balzani, V., Barigelletti, F., Campagna, S., Belser, P. and Von Zelewsky, A. 1988, Coord. Chem. Rev., 84, 85.
23. Masaoka, S., Sakai, K., 2009, Chem. Lett., 38, 182.
24. Chen, W., Rein, F. N. and Rocha, R. C. 2009, Angew. Chem. Int. Ed., 48, 9672.
25. Bonesi, S. M., Manet, I., Freccero, M., Fagnoni, M. and Albini, A. 2006, Chem. Eur. J., 12, 4844.
26. Ganesan, M., Sivasubramanian, V. K., Rajendran, T., Swarnalatha, K., Rajagopal, S. and Ramaraj, R. 2005, Tetrahedron, 61, 4863.

Entry for the Table of Contents (Please choose one layout)

Layout 1:

When water matters!
A new RuRu dyad capable of light harvesting to promote water-driven oxygenation of substrate with a marked chemoselectivity is presented

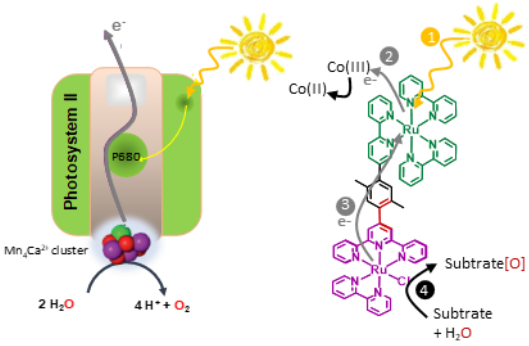

*Author(s), Corresponding Author(s)**

Page No. – Page No.

Title

Layout 2:

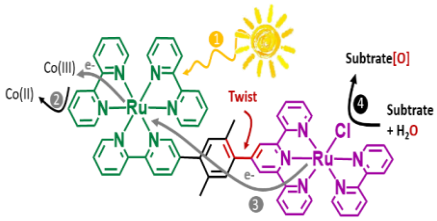

When water matters! A new RuRu dyad capable of light harvesting to promote water-driven oxygenation of substrate with a marked chemoselectivity is presented

*Author(s), Corresponding Author(s)**

Page No. – Page No.

Title

Supporting Information for

Water-assisted Photocatalytic Sulfide and Alcohol Oxidation by a Ru-Ru Dyad

J. Klein, S.Torelli,* D. Jouvenot, F. Loiseau, S. Ménage, O.Hamelin*

stephane.torelli@cea.fr, olivier.hamelin@cea.fr

Table of contents

Materials and chemicals

^{1}H NMR spectra were recorded on a Bruker Avance 300 MHz at 298K and processed with the Bruker TopSpin software. Chemical shifts (δ) are reported in parts per million (ppm) and referenced according to the applied deuterated solvent as internal standard. Coupling constants *J* are presented as absolute values in Hz. For the characterization of the NMR signals, the following abbreviations are used: s= singlet, d= doublet, t, triplet, q= quartet, m= multiplet, pst= pseudotriplet, dd= doublets of doublets, ddd= doublet of doublets of doublets).

Elemental analyses were conducted at the Institut de Chimie of Strasbourg.

Mass spectrometry spectra were recorded with a Bruker Daltonics Esquire 3000 Plus(ESI-MS) device.

Absorption spectra were recorded with a Shimadzu UV-1800 spectrophotometer.

Electrochemical experiments were performed in MeCN under inert N_2 atmosphere. A three-electrode setup was used, and consists of a glassy carbon (3mm in diameter) disk as a working electrode, a platinum wire serves as auxiliary electrode and an Ag/AgCl/ aqueous $AgCl_{sat}$ + KCl 3 M (hereafter named Ag/AgCl) as reference electrode directly dipped into the solution. Cyclic voltammograms were recorded with a Bio-logic SP-300 potentiostat piloted by the EC-Lab software. All measurements were referenced externally to ferrocene and correspond to the n+1 scan.

Emission spectra were recorded at room temperature on a Varian Cary Eclipse fluorescence spectrophotometer. Samples were placed in 1 cm path length quartz cuvettes. Luminescence lifetimes measurements were performed after irradiation at λ = 400 nm obtained by the second harmonic of a Titanium:Sapphire laser (picosecond Tsunami laser spectra physics 3950-M1BB + 39868-03 pulse picker doubler) at a 400 kHz and 8 MHz repetition rate. Fluotime 200 from AMS technologies was used for the decay acquisition. It consists of a GaAs microchannel plate photomultiplier tube (Hamamatsu model R3809U-50) followed by a time-correlated single photon counting system from Picoquant (PicoHarp300). The ultimate time resolution of the system is close to 30 ps. Luminescence decays were analyzed with Fluofit software available from Picoquant. Emission quantum yields (ϕ) were determined at room temperature in deoxygenated acetonitrile solutions using the optically dilute method. [1] $[Ru(bpy)_3]^{2+}$ (bpy = 2,2'-bipyridine) in air-equilibrated aqueous solution was used as quantum yield standard (ϕ = 0.028). [2]

The photochemical photo-oxygenation was performed in a Schlenk tube (10 mm i.d.) containing a mixture of catalyst, substrate and Co(III) salt in a 1(40μM):200:400 ratio in 0.1M phosphate buffer (pH 6.8). After 24 h of irradiation (Blue Led system emitting at 465 nm, 11mW.cm^{-2}), extraction with Et_2O (3 times) then CH_2Cl_2 (3 times) and concentration in vacuum, the products were characterized and quantified by ^1H NMR using trimethoxybenzaldehyde as internal reference.

Synthetic details

Solvents for oxygen and/or moisture sensitive reactions were freshly distilled under argon from the appropriate dehydrating agent (sodium/benzophenone "ketyl blue" for THF and CaH_2 for DMF), and degassed with dry nitrogen before use. Solvents for chromatography and work-up procedures were of puriss p.a. grade. Flash chromatography[3] was performed on silica gel (Macherey-Nagel "Silica 60 M", 40–63 μm) or aluminum oxide (deactivated by addition of 10 % water) wet-packed in glass columns. For the complexes, a puriFlash machine (30 mL/min) with prepacked columns (either 25 or 40 g) was used. $Ru(bpy)_2Cl_2 \cdot 2H_2O$ and $Ru(dmso)_4Cl_2$ were received from *Strem*. $Ru(bpy)(dmso)_2Cl_2$ was synthesized according to literature procedures.[4, 5] All other chemicals were obtained commercially and used without further purification.

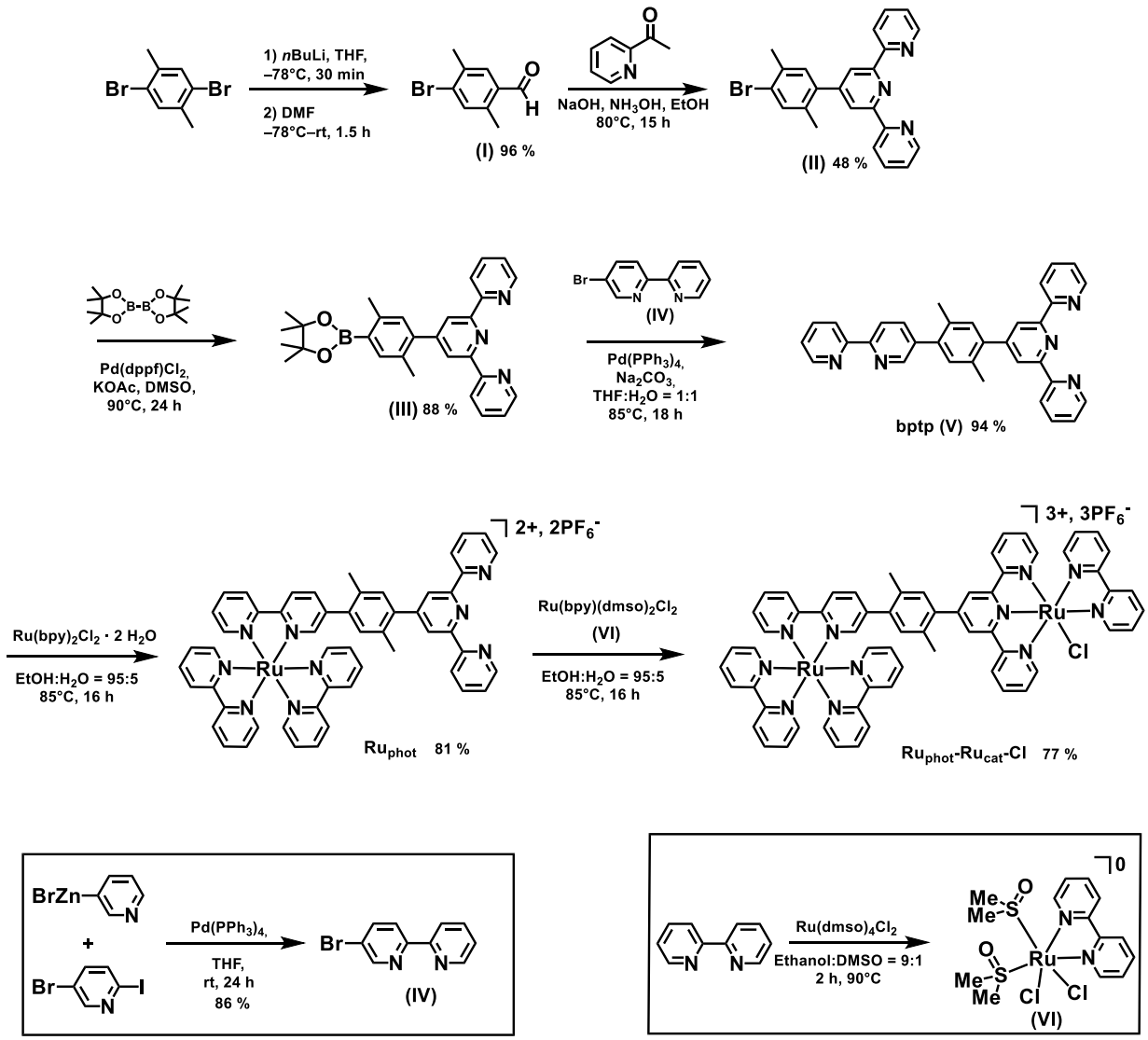

Scheme S1. Executed route to **Ru_{phot}-Ru_{cat}-Cl** *via* **Ru_{phot}**

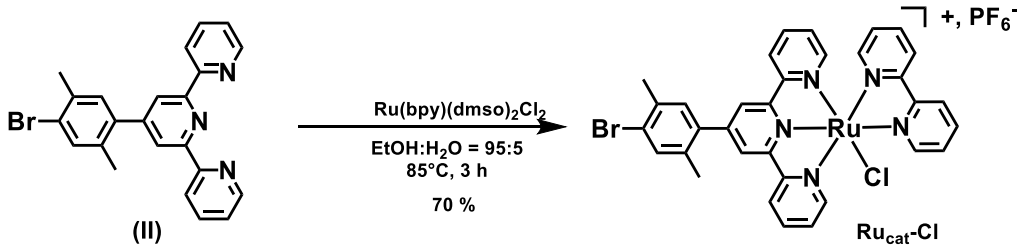

Scheme S2. Executed route to **Ru_{cat}-Cl**

4-bromo-2,5-dimethylbenzaldehyde (I). Adapted from a reported procedure. [6]

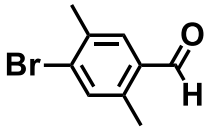

To a solution of 1,4-Dibromo-2,5-dimethylbenzene (10.6 g, 40.0 mmol) in dry THF (80 mL) , cooled to -78°C, a solution of *n*-BuLi in hexane (27.5 mL, 44.0 mmol, 1.6 M) was added. The suspension was stirred for 1.5 h at -78°C before addition of DMF (6.2 mL, 80.0 mmol). The mixture was stirred for an additional 30 min at -78°C followed by 18 h at room temperature. Aqueous NH_4OH (20 mL) was added and the two layers were separated. The aqueous phase was extracted with Et_2O (3 × 100 mL), the combined organic phases washed with water (100 mL) then brine (100 mL), extracted and dried over $MgSO_4$. After evaporation under reduced pressure, the crude product was recrystallized from hexane, dried under vacuum and **(I)** was isolated as colorless plates (8.21 g, 96 %).

^{1}H-NMR (300 MHz, C*D*Cl_3): δ =10.19 (s, 1H), 7.63 (s, 1H), 7.47 (s, 1H), 2.60 (s, 3H), 2.43 (s, 3H).

4'-(4-bromo-2,5-dimethylphenyl)-2,2':6',2''-terpyridine (II). Adapted from reported procedures. [7, 8]

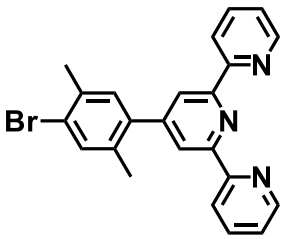

2-Acetylpyridine (1.14 g, 9.39 mmol, 1.05 mL) and NaOH (375 mg, 9.39 mmol) were mixed in a mortar and grinded for 1 min with a pestle. **(I)** (2.0 g, 9.39 mmol) was added to the yellowish solid and was grinded for 15 min until the color turned beige. Addition of the second portion 2-acetylpyridine (1.14 g, 9.39 mmol, 1.05 mL) and grinding for further 15 min results in a beige solid. The solid was dissolved in a 2:1 mixture of EtOH and aqueous solution of NH_4OH (60 mL; 25% NH_3 basis), transferred into a round bottom flask and stirred at 100°C for 2 h. The reaction mixture was cooled to room temperature and the precipitate

collected, washed with water (150 mL) to give **(II)** as a colorless solid which was used without further purification (1.59 g, 41 %).

^{1}H-NMR (300 MHz, $CDCl_3$): δ = 8.75 (ddd, J = 1.0, 1.0, 8.0 Hz, 2H), 8.71 (ddd, J = 0.9, 1.8, 4.8 Hz, 2H), 8.50 (s, 2H), 8.01 (ddd, J = 1.8, 7.6, 7.9 Hz, 2H), 7.61 (s, 1H), 7.47 (ddd, J = 1.1, 4.7, 7.5 Hz, 2H), 7.38 (s, 1H), 2.45 (s, 3H), 2.35 (s, 3H).

4'-(2,5-dimethyl-4-(4,4,5,5-tetramethyl-1,3,2-dioxaborolan-2-yl)phenyl)-2,2':6',2''-terpyridine (III). Adapted from a reported procedure. [7]

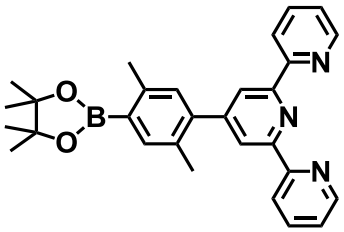

Compound **II** (1.04 g, 2.49 mmol), *bis*(pinacolato)diboron (760 mg, 2.99 mmol) and potassium acetate (734 mg, 7.48 mmol) were dissolved in dry DMSO (20 mL) under argon atmosphere and degassed for 5 min. $Pd(dppf)Cl_2$ (37.0 mg, 51.0 µmol,) was added as solid and the mixture stirred at 80°C for 18 h. Toluene (15 mL) and brine (15 mL) were added to the mixture and the phases separated. The aqueous phase was extracted with toluene (3 × 30 mL) and the combined organic layers washed with brine, dried over $MgSO_4$ and the solvent removed under reduced pressure. The crude product was purified by flash column chromatography on aluminum oxide (deactivated with 10 % water; petroleum ether) and **(III)** was obtained as a colorless solid (1.02 g, 88 %).

^{1}H-NMR (300 MHz, acetone-d_6): δ = 8.75 (ddd, J = 1.0, 1.0, 8.0 Hz, 2H), 8.70 (ddd, J = 0.9, 1.8, 4.8 Hz, 2H), 8.52 (s, 2H), 7.99 (ddd, J =1.8, 7.7, 7.7 Hz, 2H), 7.73 (s, 1H), 7.45 (ddd, J = 1.2, 4.8, 7.5 Hz, 2H), 7.22 (s, 1H), 2.57 (s, 3H), 2.35 (s, 3H), 1.38 (s, 12H).

5-Bromo-2,2´-dipyridine (IV). Adapted from a reported procedure. [9]

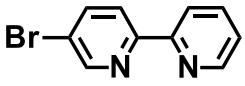

5-Bromo-2-iodopyridine (1.42 g, 5.00 mmol) was dissolved in dry THF (15 mL), degassed for 10 min and $Pd(PPh_3)_4$ (116 mg, 100 µmol) added. 2-Pyridyl zinc bromide (15.0 mL, 7.5 mmol, 0.5 M in THF) was added and the reaction mixture stirred at room temperature for 18 h. An EDTA/Na_2CO_3-solution (5 g of both compounds in 100 mL) was added and the stirring maintained until the precipitate was dissolved and the two layers separate. The aqueous phase was extracted with Et_2O (3 × 30 mL). The combined organic extracts were washed with water, dried over $MgSO_4$ and the solvent removed under reduced pressure. The residue was purified by flash column chromatography on silica (pentane:Et_2O = 2:1 (+ 0.1% NEt_3)) to give **(IV)** as beige solid (1.01 g, 86 %).

^{1}H-NMR (300 MHz, C*D*Cl_3): δ = 8.72 (dd, *J* = 0.6, 2.4 Hz, 1H), 8.67 (ddd, *J* = 0.9, 1.7, 4.8, Hz, 1H), 8.37 (ddd, *J* = 1.0, 1.0, 8.0 Hz, 1H), 8.32 (dd, *J*= 0.6, 8.5 Hz, 1H), 7.94 (dd, *J* =2.3, 8.5 Hz, 1H), 7.82 (ddd, *J* = 1.8, 7.8, 7.8 Hz, 1H), 7.32 (ddd, *J* = 1.2, 4.8, 7.5 Hz, 1H).

4'-(4-([2,2'-bipyridin]-5-yl)-2,5-dimethylphenyl)-2,2':6',2''-terpyridine bptp (V). Adapted from a reported procedure. [10]

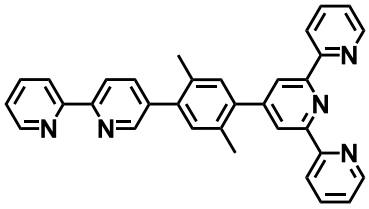

(IV) (100 mg, 425 µmol), **(III)** (217 mg, 468 µmol) and sodium carbonate (135 mg, 1.28 mmol) were dissolved in a THF:H_2O 1:1 mixture (5 mL) under argon atmosphere and degassed for 5 min. $Pd(PPh_3)_4$ (25.0 mg, 21.0 µmol) was added and the mixture was stirred at 85°C for 18 h. After cooling to room temperature, THF was removed under reduced pressure, then CH_2Cl_2 (20 mL) and water (15 mL) were added and the layers were separated. The aqueous phase was extracted with CH_2Cl_2 (3 × 30 mL) and the combined organic phase dried

over $MgSO_4$. After concentration, the crude product was purified by flash column chromatography on aluminum oxide (deactivated with 10 % water; hexane:ethyl acetate = 10:1 → 4:1 (+ NEt_3 0.1 %)) and dried under vacuum to give **(V)** as a colorless solid (197 mg, 94 %).

^{1}H-NMR (300 MHz, C*D*Cl_3): δ = 8.74–8.69 (m, 6H), 8.53 (s, 2H), 8.49 (dd, *J* = 7.8, 7.9 Hz, 2H), 7.92–7.83 (m, 4H), 7.37–7.32 (m, 4H), 7.24 (s, 1H), 2.41 (s, 3H), 2.35 (s, 3H). **^{13}C-NMR** (75 MHz, C*D*Cl_3): δ = 156.4 (C), 156.1 (C), 155.5 (C), 154.7 (C), 151.6 (C), 149.5 (CH), 149.3 (2 × CH), 139.7 (C), 138.0 (C), 137.7 (CH), 137.4 (C), 137.2 (CH), 137.1 (CH), 133.3 (C), 133.1 (C), 132.1 (CH), 131.9 (CH), 124.0 (CH), 123.9 (CH), 121.7 (CH), 121.5 (CH), 121.3 (CH), 120.7 (CH), 20.1 (CH_3), 20.0 (CH_3).

ESI-MS (m/z) (relative intensity): 514.3 (5), $\{M+Na^+\}^+$; 492.3 (100), $\{M+H^+\}^+$.

Anal. Calcd for $C_{33}H_{25}N_5$ C, 80.63; H, 5.37; N, 14.25; **found** C, 80.82; H, 5.37; N, 13.82

Ru$_{phot}$. Adapted from a reported procedure. [11]

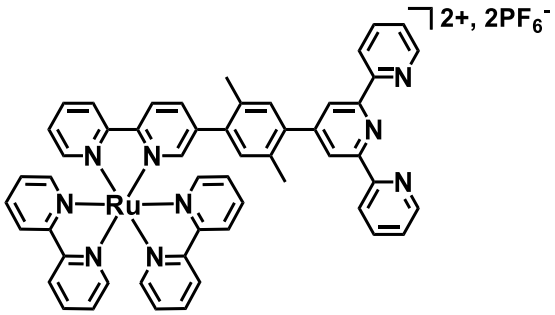

A solution of $Ru(bpy)_2Cl_2 \cdot 2H_2O$ (353 mg, 678 µmol) and **bptp** (350 mg, 712 µmol) in a 95:5 mixture of EtOH:H_2O (20 mL) was heated at 100°C for 16 h under argon. The reaction mixture was then cooled to room temperature, the solvent removed under reduced pressure and the crude product purified by flash column chromatography (eluent: acetone : water (3% KNO_3) = 9:1) on silica. The solvent of the collected fractions was removed under reduced pressure and the residue dissolved in a minimum volume of water. The product was precipitated by addition of a large excess of KPF_6 and extracted with CH_2Cl_2. The resulting organic phase was dried with Na_2SO_4 and evaporated. The resulting solid was precipitated by dropping a concentrated acetone solution of the complex into Et_2O. After filtration and vacuum drying, **Ru$_{phot}$** was collected as a red-orange solid (656 mg, 81 %).

^{1}H-NMR (300 MHz, acetone-d_6): δ 8.94 (d, J = 8.4 Hz, 1H), 8.89 (d, J = 8.1 Hz, 1H), 8.86–8.83 (m, 4H), 8.77 (ddd, J = 1.0, 1.0, 8.0 Hz, 2H), 8.72 (ddd, J = 0.9, 1.8, 4.8 Hz, 2H), 8.47 (s, 2H), 8.32 (dd, J = 2.0, 8.4 Hz, 1H), 8.29–8.17 (m, 6H), 8.15–8.09 (m, 4H), 8.06–8.00 (m, 3H), 7.66–7.56 (m, 5H), 7.49 (ddd, $^3J_{HH}$ = 1.2, 4.8, 7.5 Hz, 2H), 7.31 (s, 1H), 7.23 (s, 1H), 2.33 (s, 3H), 2.10 (s, 3H). **^{13}C-NMR** (75 MHz, acetone-d_6): δ = 158.3 (C), 158.19 (C), 158.18 (C), 158.16 (C), 158.05 (C), 156.7 (C), 156.5 (C), 153.0 (CH), 152.90 (CH), 152.86 (CH), 152.83 (CH), 152.76 (CH), 152.1 (CH), 151.5 (C), 150.2 (CH), 141.4 (C), 139.4 (CH), 139.08 (CH), 139.06 (CH), 139.0 (CH), 138.1 (CH), 136.3 (C), 134.2 (C), 134.1 (C), 133.0 (CH), 132.7 (CH), 128.92 (CH), 128.86 (CH), 128.83 (CH), 128.81 (CH), 128.75 (CH), 125.5 (CH), 125.40 (CH), 125.36 (CH), 125.20 (CH), 125.16 (CH), 121.9 (CH), 121.7 (CH), 19.9 (CH_3), 19.8 (CH_3).

ESI-MS (m/z) (relative intensity): 452.8 (100), $\{M\text{-}2PF_6^-\}^{2+}$; 302.1 (7), $\{M\text{-}2PF_6^-+H^+\}^{3+}$.

Ru(bpy)(dmso)$_2$Cl$_2$ (VI). Adapted from a reported procedure. [12]

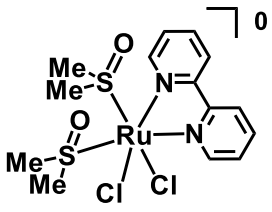

A solution of *cis*-Ru(dmso)$_4$Cl$_2$ (100 mg, 206 µmol) and 2,2´-dipyridine (32.0 mg, 206 µmol) in a mixture of EtOH:DMSO = 9:1 (10 mL) was stirred for 2 h at 85°C. After cooling to room temperature, a mixture of AcOEt:Et$_2$O = 1:3 (20 mL) was added and the resulting precipitate collected, washed with a mixture of AcOEt:Et$_2$O = 1:3 (20 mL) and vacuum dried, yielding **(VI)** as a pale yellow solid (78 mg, 78 %).

^{1}H-NMR (300 MHz, C*D*Cl$_3$): δ = 9.89 (d, J = 7.0 Hz, 1H), 9.72 (d, J = 5.9 Hz, 1H), 8.16 (d, J = 7.9 Hz, 1H), 8.11 (d, J = 7.9 Hz, 1H), 8.00 (dd, J = 8.1, 8.1 Hz, 1H), 7.89 (dd, J = 7.7, 7.7 Hz, 1H), 7.60 (dd, J = 6.6, 6.6 Hz, 1H), 7.45 (dd, J = 6.6, 6.6 Hz, 1H), 3.56 (s, 3H), 3.52 (s, 3H), 3.21 (s, 3H), 2.65 (s, 3H).

Ru_{cat}-Cl. Adapted from reported procedures. [13-15]

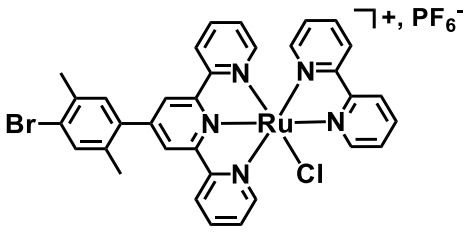

A solution of Ru(bpy)(dmso)$_2$Cl$_2$ (58.0 mg, 120 µmol) and **(II)** (50.0 mg, 120.0 µmol) in a mixture of EtOH:H_2O = 95:5 (10 mL) was stirred under argon at 100°C for 16 h. The mixture was cooled to room temperature, the solvents removed under reduced pressure and the crude product purified by flash column chromatography on silica (eluent: acetone:water (3% KNO_3) = 9.5:0.5). After concentration in vacuo, the resulting solid was dissolved in MeOH with a minimum volume of acetone for complete solubility. Insoluble KNO_3 salt was filtered off and the solvent removed under reduced pressure. The red solid was dissolved in CH_2Cl_2 and successively washed with saturated aqueous KPF_6 solution (2 × 20 mL) and water. The solution was dried with Na_2SO_4 and the solvents evaporated under reduced pressure. The resulting solid was dissolved in a minimum amount of acetone and dropped into Et_2O to precipitate and give **Ru_{cat}-Cl** as a deep red solid (72 mg, 70 %).
Single crystals suitable for X-ray crystallography were grown by diffusion of pentane into a concentrated solution of **Ru_{cat}** in acetone.

^{1}H-NMR (300 MHz, acetone-d6): δ = 10.37 (d, J = 5.1 Hz, 1H), 8.88 (d, J = 8.2 Hz, 1H), 8.75-8.71 (m, 4H), 8.61 (d, J = 8.6 Hz, 1H), 8.39 (dd, J = 7.6, 7.9 Hz, 1H), 8.08 (dd, J = 6.4, 6.4 Hz, 1H), 8.00 (dd, J = 7.8, 7.9 Hz, 2H), 7.86-7.79 (m, 3H), 7.70 (s, 1H), 7.67 (d, J = 5.3 Hz, 1H), 7.61 (s, 1H), 7.41 (dd, J = 6.2, 6.9 Hz, 2H), 7.11 (dd, J = 5.7, 6.8 Hz, 1H), 2.55 (s, 3H), 2.49 (s, 3H). **^{13}C-NMR** (75 MHz, acetone-d_6): δ =159.00 (C), 158.93 (C), 157.92 (C), 156.37 (C), 152.73 (CH), 152.25 (CH), 152.11 (CH), 146.14 (C), 137.94 (C), 136.87 (CH), 136.59 (CH), 135.68 (C), 135.54 (CH), 135.43 (C), 134.28 (CH), 132.26 (CH), 127.28 (CH), 126.79 (CH), 126.29 (CH), 124.97 (C), 123.70 (CH), 123.48 (CH), 123.32 (CH), 122.72 (CH), 21.49 (CH_3), 18.92 (CH_3).

ESI-MS (m/z) (relative intensity): 710.1 (100%), $\{M\text{-}PF_6^-\}^+$

Ru_{phot}-Ru_{cat}-Cl. Adapted from reported procedures. [13-15]

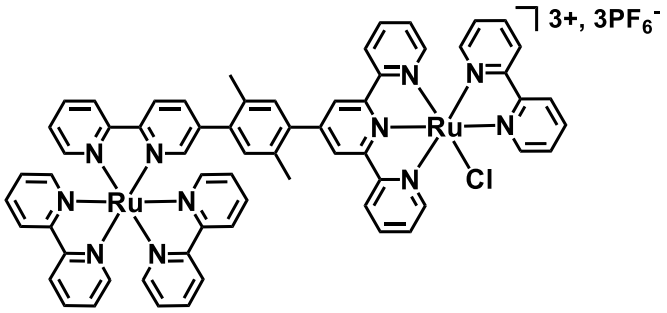

A solution of Ru(bpy)$(dmso)_2Cl_2$ (50.0 mg, 103 µmol) and **Ru_{phot}** (123 mg, 103 µmol) in a mixture of EtOH:H_2O = 95:5 (10 mL) was stirred under inert atmosphere at 100°C for 16 h. After concentration under reduced pressure, the crude product was purified by flash column chromatography on silica (acetone:water (3% KNO_3) = 4:1). The residue was dissolved in MeOH with a minimum volume of acetone for complete solubility and KNO_3 filtered off. After evaporation and dissolution in CH_2Cl_2, the organic layer was washed with a saturated aqueous KPF_6 solution (2 × 20 mL) and water. The organic layer was dried with Na_2SO_4 and the solvent evaporated. Deep red **Ru_{phot}-Ru_{cat}-Cl** was precipitated by dropping a concentrated acetone solution of the complex into Et_2O (136 mg, 81 %).

^{1}H-NMR (300 MHz, acetone-d_6): δ 10.36 (d, 4.8 Hz, 1H), 8.80-9.00 (m, 8H), 8.69 (pst, 4.1Hz, 4H), 8.61 (d, 8.1Hz, 1H), 8.40 (t, 7.8 Hz, 1H), 8.35 (dd, 8.4, 2.0 Hz, 1H), 8.20-8.32 (m, 7H), 8.03-8.20 (m, 7H), 7.99 (dt, 7.8, 1.5Hz, 2H), 7.53-7.70 (m, 8H), 7.41 (ddd, 5.7, 5.4, 0.9 Hz, 2H), 7.35 (s, 1H), 7.11 (t, 7.5Hz, 1H), 2.55 (s, 3H), 2.15 (s, 3H). **^{13}C-NMR** (75 MHz, acetone-d_6): δ 158.94 (C), 158.86 (C), 157.92 (C), 157.46 (C), 157.30 (C), 157.27 (C), 157.24 (C), 157.12 (C), 156.35 (C), 155.92 (C), 152.68 (CH), 155.22 (CH), 152.04 (CH), 151.98 (CH), 151.93 (CH), 151.87 (CH), 151.03 (CH), 146.21 (C), 140.34 (C), 139.30 (C), 138.58 (CH), 138.23 (CH), 138.16 (CH),136.86 (CH), 136.61 (CH), 135.95 (C), 135.56 (CH), 134.07 (C), 133.27 (C),132.63 (CH), 132.32 (CH), 128.08 (CH),, 128.00 (CH),, 127.91 (CH),127.90 (CH), 127.29 (CH), 126.76 (CH),126.31 (CH), 124.90 (C), 124.60 (CH),124.50 (CH),124.44 (CH), 124.35 (CH), 123.71 (CH), 123.48 (CH), 123.31 (CH), 122.60 (CH), 19.09 (CH_3), 19.01 (CH_3).

ESI-MS (m/z) (relative intensity): 671.5 (15%), $\{M\text{-}2PF_6^-\}^{2+}$; 399.3 (100), $\{M\text{-}3PF_6^-\}^{3+}$.

Anal. Calcd for $C_{63}H_{49}N_{11}Ru_2ClP_3F_{18}$, $5H_2O$: C, 43.92; H, 3.45; N, 8.94; **found**C, 43.54; H, 2.99; N, 8.99.

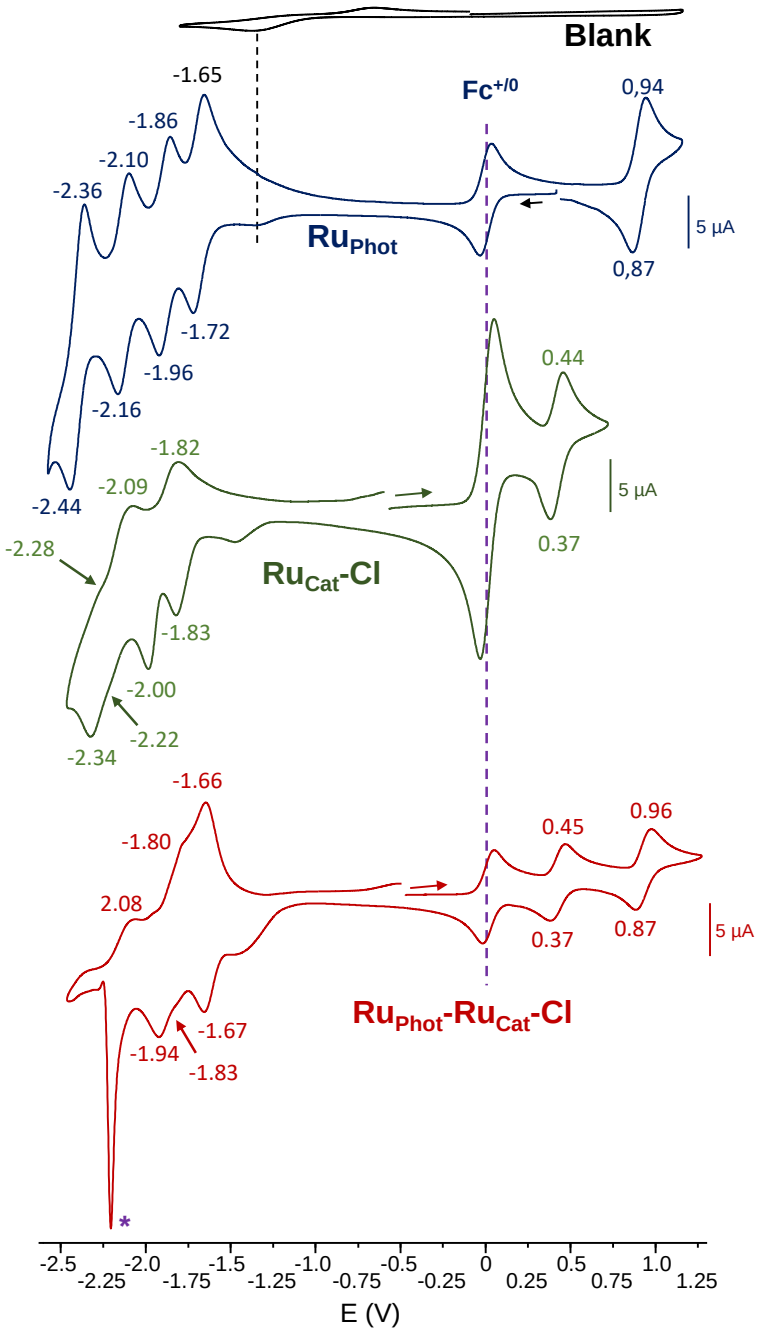

Figure S1. Cyclic voltammograms of 1 mM $\mathbf{Ru^{II}_{phot}}$ (in blue), $\mathbf{Ru_{cat}}$**-Cl** (in green) and $\mathbf{Ru^{II}_{phot}}$-$\mathbf{Ru^{II}_{cat}}$**-Cl** (in red) recorded in acetonitrile; Ag/AgCl as reference electrode, glassy carbon as working electrode; 0.1 M $(nBu)_4NPF_6$, 100 $mV.s^{-1}$. *denotes chemical adsorption at the working electrode.

Table S1. Crystal data and structure refinement for **Ru_{cat}-Cl**.

Empirical formula	**$C_{35.84}H_{31.54}BrClF_6N_{5.16}O_{0.84}PRu$**
Formula weight	909.43
Temperature	150(1) K
Wavelength	0.71073 Å
Crystal system	Monoclinic
Space group	$P2_1/c$
Unit cell dimensions	a = 8.6264(7) Å α = 90.00° b = 21.788(2) Å β = 96.969(5)° c = 19.5229(11) Å γ = 90.00°
Volume, Z	3642.3(5) $Å^3$, 4
Density (calculated)	1.658 g/cm^3
Absorption coefficient	1.713 mm^{-1}
F(000)	1818.0
Crystal size	0.947 x 0.054 x 0.027 mm
θ range for data collection	4.28° to 52.74°
Limiting indices	$-7\leq h\leq 10$, $-27\leq k\leq 25$, $-24\leq l\leq 24$
Reflections collected	16711
Independent reflections	7448 [R(int) = 0.0619
Absorption correction	Semi-empirical from equivalents
Refinement method	Full-matrix least-squares on F^2
Data / Restraints / Parameters	7448 / 260 / 818
Goodness-of-fit on F^2	1.035
Final R indices [$I>2\sigma(I)$]	R1 = 0.0519, wR2 = 0.0939
R indices (all data)	R1 = 0.0927, wR2 = 0.1086

Table S2. Bond lengths for **Ru_{cat}-Cl**.

Atom	Atom	Length/Å	Atom	Atom	Length/Å
Ru1	Cl1	2.4112(12)	C32	C33	1.378(7)
Ru1	N1	2.056(3)	C33	C34	1.380(7)
Ru1	N2	1.951(3)	C34	C35	1.383(7)
Ru1	N3	2.072(3)	C35	C36	1.474(6)
Ru1	N31	2.028(4)	C36	C37	1.385(6)
Ru1	N32	2.066(3)	C37	C38	1.367(7)
Br3	Br2	0.774(12)	C38	C39	1.363(7)
Br3	C19B	1.94(2)	C39	C40	1.373(6)
Br3	Br1	0.72(3)	Br2	C19B	1.92(2)
Br3	C19	1.886(11)	C16B	C17B	1.35(4)
N1	C1	1.339(5)	C16B	C21B	1.34(4)
N1	C5	1.361(5)	C17B	C18B	1.41(4)
N2	C6	1.350(5)	C17B	C22B	1.56(4)
N2	C10	1.362(5)	C18B	C19B	1.35(3)
N3	C11	1.371(5)	C19B	C20B	1.34(3)
N3	C15	1.341(5)	C20B	C21B	1.49(4)
N31	C31	1.344(5)	C20B	C23B	1.54(3)
N31	C35	1.354(5)	Br1	C19	1.915(8)
N32	C36	1.360(6)	C16	C17	1.388(15)
N32	C40	1.344(6)	C16	C21	1.421(11)
C1	C2	1.380(6)	C17	C18	1.403(13)
C2	C3	1.370(6)	C17	C22	1.471(13)
C3	C4	1.378(6)	C18	C19	1.364(11)
C4	C5	1.395(6)	C19	C20	1.389(11)
C5	C6	1.479(6)	C20	C21	1.353(12)
C6	C7	1.384(6)	C20	C23	1.546(11)
C7	C8	1.399(6)	C41	O41	1.190(11)

C8	C9	1.400(6)	C41	C42	1.457(11)
C8	C16B	1.38(5)	C41	C43	1.491(11)
C8	C16	1.522(15)	C41	N41	1.27(7)
C9	C10	1.369(6)	C41	C44	1.382(19)
C10	C11	1.472(6)	P1	F1	1.591(3)
C11	C12	1.377(6)	P1	F2	1.591(3)
C12	C13	1.364(7)	P1	F3	1.585(4)
C13	C14	1.378(6)	P1	F4	1.601(3)
C14	C15	1.387(6)	P1	F5	1.588(4)
C31	C32	1.365(7)	P1	F6	1.590(3)

Table S3. Bond angles for **Ru_{cat}-Cl**.

Atom	**Atom**	**Atom**	**Angle/°**	**Atom**	**Atom**	**Atom**	**Angle/°**
N1	Ru1	Cl1	90.30(11)	C34	C35	C36	124.0(4)
N1	Ru1	N3	159.21(14)	N32	C36	C35	113.7(4)
N1	Ru1	N32	99.04(13)	N32	C36	C37	121.4(4)
N2	Ru1	Cl1	88.67(11)	C37	C36	C35	124.9(4)
N2	Ru1	N1	79.71(14)	C38	C37	C36	119.5(5)
N2	Ru1	N3	79.63(14)	C39	C38	C37	119.6(5)
N2	Ru1	N31	98.00(14)	C38	C39	C40	118.9(5)
N2	Ru1	N32	176.54(15)	N32	C40	C39	123.2(5)
N3	Ru1	Cl1	91.53(11)	Br3	Br2	C19B	79.7(14)
N31	Ru1	Cl1	173.32(10)	C17B	C16B	C8	131(3)
N31	Ru1	N1	91.22(14)	C21B	C16B	C8	113(3)
N31	Ru1	N3	89.36(14)	C21B	C16B	C17B	115(3)
N31	Ru1	N32	78.77(14)	C16B	C17B	C18B	126(3)
N32	Ru1	Cl1	94.57(11)	C16B	C17B	C22B	123(3)
N32	Ru1	N3	101.46(13)	C18B	C17B	C22B	110(3)
Br2	Br3	C19B	77.2(15)	C19B	C18B	C17B	117(2)
Br2	Br3	C19	101.3(13)	Br2	C19B	Br3	23.1(4)
Br1	Br3	Br2	174.7(14)	C18B	C19B	Br3	132(2)
Br1	Br3	C19B	105.2(15)	C18B	C19B	Br2	110(2)
Br1	Br3	C19	81.4(11)	C20B	C19B	Br3	106(2)
C19	Br3	C19B	24.1(8)	C20B	C19B	Br2	128(2)
C1	N1	Ru1	128.7(3)	C20B	C19B	C18B	122(2)
C1	N1	C5	117.9(4)	C19B	C20B	C21B	117(2)
C5	N1	Ru1	113.4(3)	C19B	C20B	C23B	131(2)
C6	N2	Ru1	119.2(3)	C21B	C20B	C23B	111(2)
C6	N2	C10	121.4(4)	C16B	C21B	C20B	122(3)
C10	N2	Ru1	119.3(3)	Br3	Br1	C19	76.9(6)

C11	N3	Ru1	113.2(3)	C17	C16	C8	121.7(7)
C15	N3	Ru1	127.8(3)	C17	C16	C21	119.5(10)
C15	N3	C11	118.9(4)	C21	C16	C8	118.8(10)
C31	N31	Ru1	125.0(3)	C16	C17	C18	117.6(8)
C31	N31	C35	118.4(4)	C16	C17	C22	124.6(9)
C35	N31	Ru1	116.5(3)	C18	C17	C22	117.7(10)
C36	N32	Ru1	115.8(3)	C19	C18	C17	120.8(8)
C40	N32	Ru1	126.8(3)	Br3	C19	Br1	21.8(8)
C40	N32	C36	117.4(4)	C18	C19	Br3	100.2(11)
N1	C1	C2	122.2(4)	C18	C19	Br1	119.6(7)
C3	C2	C1	119.7(4)	C18	C19	C20	122.7(8)
C2	C3	C4	119.6(4)	C20	C19	Br3	136.8(10)
C3	C4	C5	118.1(4)	C20	C19	Br1	117.5(6)
N1	C5	C4	122.4(4)	C19	C20	C23	123.9(7)
N1	C5	C6	115.3(4)	C21	C20	C19	116.9(8)
C4	C5	C6	122.2(4)	C21	C20	C23	119.2(7)
N2	C6	C5	112.2(4)	C20	C21	C16	122.4(9)
N2	C6	C7	120.1(4)	O41	C41	C42	118.4(10)
C7	C6	C5	127.8(4)	O41	C41	C43	120.2(9)
C6	C7	C8	120.1(4)	O41	C41	N41	29(3)
C7	C8	C9	117.7(4)	O41	C41	C44	159(3)
C7	C8	C16	123.8(6)	C42	C41	C43	121.4(8)
C9	C8	C16	118.3(6)	N41	C41	C42	117(4)
C16B	C8	C7	114.1(17)	N41	C41	C43	114(4)
C16B	C8	C9	127.9(17)	N41	C41	C44	156(4)
C16B	C8	C16	13.5(17)	C44	C41	C42	44(2)
C10	C9	C8	120.8(4)	C44	C41	C43	78(3)
N2	C10	C9	119.8(4)	F1	P1	F4	90.03(18)
N2	C10	C11	112.4(4)	F2	P1	F1	179.2(2)
C9	C10	C11	127.8(4)	F2	P1	F4	90.05(17)

N3	C11	C10	115.2(4)	F3	P1	F1	90.27(18)
N3	C11	C12	120.5(4)	F3	P1	F2	90.5(2)
C12	C11	C10	124.3(4)	F3	P1	F4	89.8(2)
C13	C12	C11	120.6(4)	F3	P1	F5	179.7(2)
C12	C13	C14	119.1(4)	F3	P1	F6	89.8(2)
C13	C14	C15	119.1(4)	F5	P1	F1	89.4(2)
N3	C15	C14	121.8(4)	F5	P1	F2	89.79(19)
N31	C31	C32	122.8(4)	F5	P1	F4	90.2(2)
C31	C32	C33	119.3(5)	F5	P1	F6	90.2(2)
C32	C33	C34	118.4(5)	F6	P1	F1	90.21(18)
C33	C34	C35	120.1(5)	F6	P1	F2	89.72(18)
N31	C35	C34	120.8(4)	F6	P1	F4	179.6(2)
N31	C35	C36	115.2(4)				

References

1. Crosby G. A. and Demas J. N., 1971, J. Phys. Chem.,75, 991.
2. Nakamaru N., 1982, Bull. Chem. Soc. Jpn., 55, 2697.
3. Still W. C., Kahn M. and Mitra A., 1978, J. Org. Chem., 43, 2923.
4. Mari T., Ken-ichi I., Shinobu I. and Noriharu N., 2006, Bull. Chem. Soc. Jpn., 79, 1525.
5. Tong L., Inge A. K., Duan L., Wang L., Zou X. and Sun L., 2013, Inorg. Chem., 52, 2505.
6. Liang T.-C. and Lin H.-C. 2009, Journal of Polymer Science: Part A: Polymer Chemistry, , 47, 2734.
7. Farran R., Jouvenot D., Gennaro B., Loiseau F., Chauvin J. and Deronzier A. 2016, ACS Appl. Mater. Interfaces, 8, 16136.
8. Cavea G. W. V. and Raston C. L. 2001, J. Chem. Soc. Perk. Trans 2, 3258.
9. Heinz L. G., Yushchenko O., Neuburger M., Vauthey E. and Wenger O. S., 2015, J. Phys. Chem. A, 119, 5676.
10. Orazietti M., Kuss-Petermann M., Hamm P. and Wenger O. S., 2016, Angew. Chem. Int. Ed., 55, 9407.
11. Hamelin O., Rimboud M., Pécaut J. and Fontecave M., 2007, Inorg. Chem., 46, 5354.
12. Evans P., Spencer A. and Wilkinson G., 1973, J. Chem. Soc. Dalton Trans., 2, 204.
13. Odobel F. and Zabri H., 2005, Inorg. Chem., 44, 5600.
14. Nair N. V., Zhou R. and Thummel R. P., 2017, Inorg. Chim. Acta, 454, 27.
15. Hamelin O., Guillo P., Loiseau F., Boissonnet M.-F. and Ménage S., 2011, Inorg. Chem., 50, 7952